VIII International Conference on Computational Methods for Coupled Problems in Science and Engineering
COUPLED PROBLEMS 2019
E. Oñate, M. Papadrakakis and B. Schrefler (Eds)

PRESTRESSED VIBRATIONS OF PARTIALLY FILLED TANKS CONTAINING A FREE-SURFACE FLUID: FINITE ELEMENT AND REDUCED ORDER MODELS

C. HOAREAU*, J.-F. DEÜ* AND R. OHAYON*

*Laboratoire de Mécanique des Structures et des Systèmes Couplées (LMSSC)
Conservatoire national des arts et métiers (Cnam), 292 Rue Saint-Martin, Paris 75003, France
e-mail: {christophe.hoareau, jean-francois.deu, roger.ohayon}@lecnam.net, web page: http://www.lmssc.cnam.fr/en

Key words: reduced order model, hydroelasticity, geometrical nonlinearity, prestressed vibrations, finite elements

Abstract. In linear vibration analysis of partially filled elastic tanks [1], even if the the structure is submitted by a gaz or a liquid pressure, the reference configuration is generally used without the effect of static loads. In the case of very thin structures or soft material, the static state is considered as prestressed, due to geometrical nonlinearities of the deformed tank. The global stiffness of the structure may change in function of the fluid volume amount [2, 3, 4]. The aim of the paper is to quantify the prestressed effets on the linearized dynamic behavior of the fluid-structure system. The chosen methodology is the following: (i) A quasi-static solution is computed from an empty to a fully filled state of the tank, by considering geometrical nonlinearities and hydrostatic follower forces [5] (no volumetric mesh of the fluid is needed for this step); (ii) after a volumetric remeshing of the fluid at each states, a linearized hydroelastic displacement-pressure formulation around the prestressed state, without gravity effects, is established; (iii) a reduced basis of the hydroelastic problem is generated by using prestressed dry modes to minimize the computation of the added mass matrix. Numerical examples are given to illustrate the proposed approaches.

1 INTRODUCTION

For geometrical simple fluid-structure systems such as cylinders, relevant of semi-analytical analysis, the problem has been solved by using, as a projection basis, the structural dry modes (i.e. modes *in vacuo*).

For complex structures, it is known that the presence of an added mass operator may lead to prohibitive computational times and memory (computation of a Schur complement matrix). An alternative formulation, for partially filled structures, using the computation of the added mass for a limited number of filled structures, has been presented in [1]. In the paper, the aim is to evaluate here the approach using only dry-structural modes, but prestressed, in order to reduce future computational times.

1.1 Definition of the emptying rate

We consider an elastic tank partially filled by an internal fluid. We denote by V_t the initial volume tank and V_f the current fluid volume corresponding to various level of liquid in the tank. We define the emptying rate τ such that

$$\tau = \frac{V_\mathrm{t} - V_\mathrm{f}}{V_\mathrm{t}} \tag{1}$$

The main objective of the study is to estimate the influence of this parameter on the prestressed dynamic behavior of the fluid-structure system. We make the assumption that the frequency range of interest is high enough ($f > 5$ Hz) compared to the evolution of the emptying rate, so the evolution of the fluid volume is supposed to be quasi-static in our study. Thereby, at each emptying rate the fluid-structure system vibrations are computed around a quasi-static equilibrium state.

1.2 Fluid-structure-hypotheses

Structure - In the numerical examples, the structure is supposed to be isotropic, homogeneous, elastic and prestressed. At the equilibrium, the displacements of the structure are high enough to take into account the prestressed effect on the dynamic behavior due to an hydrostatic or a gas pressurization. The linear vibrations are computed around each prestressed configurations. Three states of the structural domain, described in Fig. 1, are considered. At first, the reference configuration Ω_0 is the domain occupied by the solid without any external forces. The associated position vector is noted $\mathbf{X}_0$. Then, the current "quasi-static" Ω_q is the domain occupied by the structure considering finite deformations. The position of the prestressed state is associated with $\mathbf{x}_\mathrm{q} = \mathbf{X}_0 + \mathbf{u}_\mathrm{q}$. Finally, we denote Ω_s the current "dynamic" configuration under the assumption of harmonic excitations and the position vector $\mathbf{x}_\mathrm{s} = \mathbf{x}_\mathrm{q} + \mathbf{u}_\mathrm{s}$. In the following, Ω_s and Ω_q coincide because $\|\mathbf{u}_\mathrm{s}\|$ is very small compared the thickness t of the elastic tank. All the domains are bounded of $\mathbb{R}^3$.

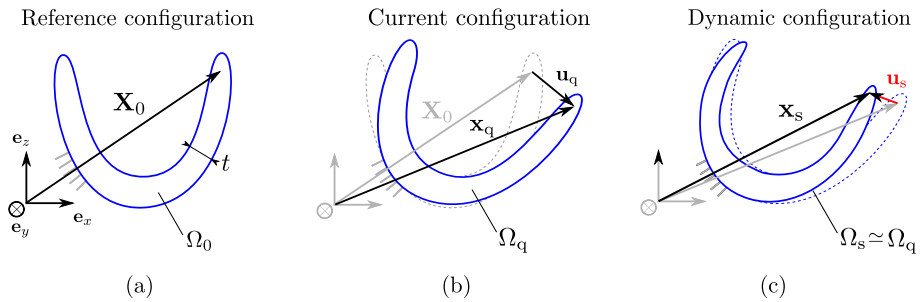

Figure 1: (a) Reference configuration for a dry structure; (b) Current "quasi-static" configuration in finite deformation; (c) Linearized "structural" dynamic configuration around the prestressed state.

Free-surface fluid hypotheses - At the equilibrium, the horizontal free-surface fluid is supposed to be at rest, homogeneous, inviscid, incompressible and without surface tension. We neglect, as usually done in hydroelastic linear vibrations, the gravity effect (sloshing). Consequently, the pressure fluctuation is null on the free-surface Γ and written as

$$p = 0 \quad \text{on} \quad \Gamma \tag{2}$$

Finally, we denote by Σ the fluid-structure interface on the current configuration. The Fig. 2 recapitulates the methodology such that:

- Phase 1: Computation of the quasi-static deformation in finite deformation;
- Phase 2: Coincident re-meshing of the fluid and the structure around the prestressed state;
- Phase 3: Prestressed hydroelastic vibrations

Only Phase 3 will be presented in the current paper.

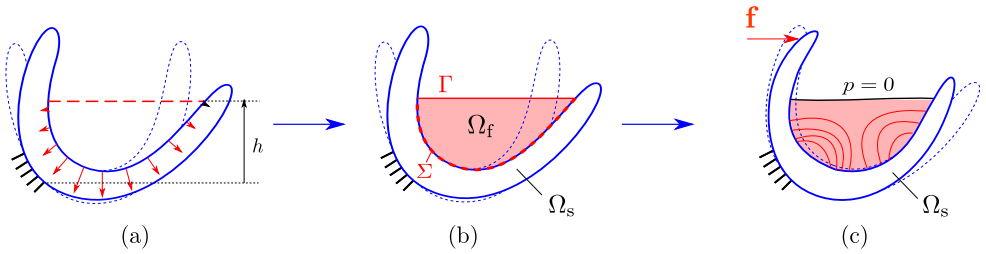

Figure 2: (a) Phase 1: Prestressed state computed with follower forces (due to a gas or liquide pressure); (b) Phase 2: Current configuration of the structure Ω_q around a quasi-static equilibrium and the fluid domains Ω_f at rest; (c) Phase 3: Hydroelastic vibrations around the prestressed state with an excitation $\mathbf{f}$ and a pressure fluctuation $p = 0$ on the free surface Γ

2 Discretized added mass prestressed hydroelastic formulation

In this section, the nodal finite element displacement $\mathbf{U}_\mathrm{q}$ of a deformed elastic structure, related to the quasi-static finite deformation, is supposed to be known. We denote by $\mathbf{U}_\mathrm{s}$ the fluctuation of displacement vector around the prestressed state. The structure is supposed to be clamped at $\partial_\mathrm{u}\Omega_0 = \partial_\mathrm{u}\Omega_\mathrm{s}$.

2.1 Symmetric eigenvalue problem with added mass matrix

We will use an intermediate discrete variable called the fluid displacement potential, denoted by $\boldsymbol{\varphi}$, related to the pressure fluctuation vector $\mathbf{P}$ by $\mathbf{P} = \rho_\mathrm{f}\omega^2\boldsymbol{\varphi}$ (with $\boldsymbol{\varphi} = \mathbf{0}$ on Γ). Using the condition of $\mathbf{P}$ or $\boldsymbol{\varphi}$, the discretized variational approach of the FSI problem leads to a pure structural eigenvalue problem written as

$$[\mathbf{K}_\mathrm{tan} - \omega^2(\mathbf{M} + \mathbf{M}_\mathrm{a})]\mathbf{U}_\mathrm{s} = \mathbf{0} \tag{3}$$

$$\mathbf{M}_\mathrm{a} = \rho_\mathrm{f}\mathbf{C}_*\mathbf{H}_*^{-1}\mathbf{C}_*^\mathrm{T} \tag{4}$$

where ρ_f is the fluid density, $*$ corresponds to the matrices which take into account $\boldsymbol{\varphi} = \mathbf{0}$ on Γ and:

- $\mathbf{K}_\mathrm{tan}$ is the tangent stiffness matrix which is symmetric and supposed to be positive-definite. The tangent matrix is a contribution of the geometrical, material and load contribution to the stiffness of the prestressed structure, respectively denoted by $\mathbf{K}_\mathrm{g}$, $\mathbf{K}_\mathrm{m}$ and $\mathbf{K}_\mathrm{f}$, such that:

$$\mathbf{K}_\mathrm{tan} = \mathbf{K}_\mathrm{g} + \mathbf{K}_\mathbf{m} + \mathbf{K}_\mathrm{f} \tag{5}$$

- $\mathbf{M}$ is the positive-definite mass matrix of the structure;
- $\mathbf{M}_\mathrm{a}$ is the added mass matrix which is positive-definite, symmetric and full in the columns and the lines related to the fluid-structure interface displacements degrees of freedom;
- $\mathbf{H}$ is a fluid operator related to the kinetic energy of the displaced fluid induced by the displacement of the fluid-structure interface;
- $\mathbf{C}$ is the coupling matrix at the fluid-structure interface.

We shall note that $\mathbf{K}_\mathrm{tan}$, $\mathbf{M}$, $\mathbf{C}$ and $\mathbf{H}$ depend on the known quasi-static displacement $\mathbf{U}_\mathrm{q}$. The eigenvalues and eigenvectors of the system Eq. (3) are respectively the prestressed hydroelastic natural angular frequencies ω_α and the structural part of the hydroelastic modes $\mathbf{U}_\alpha$. Due to the fluid incompressibility and geometric considerations from the fluid-structure interface displacements, the potential of displacement part is then deduced, for each hydroelastic modes, with the following equations:

$$\mathbf{H}_*\boldsymbol{\varphi}_\alpha = -\mathbf{C}_*^\mathrm{T}\mathbf{U}_\alpha \tag{6}$$

Due to the matrix inverse computation $\mathbf{H}_*^{-1}$ in Eq. (4), the computational time might become prohibitive.

3 PROJECTION ON PRESTRESSED DRY MODES

The projection of the coupled problem on the dry modes is presented in three steps :

Step 1: We compute N eigenvectors by solving the linearized eigenvalue problem of the structure *in vacuo*:

$$[\mathbf{K}_{\text{tan}} - \omega^2 \mathbf{M}]\mathbf{U}_{\text{s}} = \mathbf{0} \tag{7}$$

Step 2: For each deformed shapes $\mathbf{U}_\beta$, we solve a linear system to compute the associated fluid potential displacement [1] expressed as:

$$\mathbf{H}_* \boldsymbol{\varphi}_\beta = -\mathbf{C}_*^{\text{T}} \mathbf{U}_\beta \tag{8}$$

where $\boldsymbol{\varphi}_\beta$ is the associated fluid potential displacement ($\boldsymbol{\varphi}_\beta = \mathbf{0}$ on the discretized free surface Γ). We introduce the following notations:

$$\mathbf{B} = \begin{bmatrix} \vdots & & \vdots \\ \mathbf{U}_1 & \dots & \mathbf{U}_N \\ \vdots & & \vdots \end{bmatrix}, \qquad \boldsymbol{\Phi} = \begin{bmatrix} \vdots & & \vdots \\ \boldsymbol{\varphi}_1 & \dots & \boldsymbol{\varphi}_N \\ \vdots & & \vdots \end{bmatrix} \quad \text{and} \quad \boldsymbol{\kappa} = \begin{bmatrix} \kappa_1 \\ \vdots \\ \kappa_N \end{bmatrix} \tag{9}$$

where $\mathbf{B}$ and $\boldsymbol{\Phi}$ are the rectangular matrices containing respectively each structural eigenvectors (normalized by the mass matrix $\mathbf{M}$) and the associated potential of displacements on the fluid for each mode. $\boldsymbol{\kappa}$ is the generalized unknown coordinates vector. We suppose that N is high enough such that $\mathbf{U}_{\text{s}} \simeq \mathbf{B}\kappa$.

Step 3: The induced pressure associated with the β^{th} dry mode is written in the following form:

$$\mathbf{P}_\beta = -\omega^2 \rho_{\text{f}} \boldsymbol{\varphi}_\beta \boldsymbol{\kappa}_\beta \tag{10}$$

We take into account each pressure contribution of the fluid, induced by the structural dry modes displacements such that an external load appear in the right side of Eq. (7) written as:

$$[\mathbf{K}_{\text{tan}} - \omega^2 \mathbf{M}]\mathbf{B}\boldsymbol{\kappa} = \omega^2 \rho_{\text{f}} \mathbf{C} \boldsymbol{\Phi} \boldsymbol{\kappa} \tag{11}$$

Finally by multiplying Eq. (11) by $\mathbf{B}^{\text{T}}$ in the left, we obtain the following reduced eigenvalue equation:

$$[\boldsymbol{\Omega} - \omega^2 (\mathbf{I} + \mathbf{r}_{\text{a}})]\boldsymbol{\kappa} = \mathbf{0} \tag{12}$$

where $\boldsymbol{\Omega} = \mathbf{B}^{\text{T}} \mathbf{K}_{\text{tant}} \mathbf{B}$, $\mathbf{I} = \mathbf{B}^{\text{T}} \mathbf{M} \mathbf{B}$ and $\mathbf{r}_{\text{a}} = \rho_{\text{f}} \mathbf{B}^{\text{T}} \mathbf{C}^{\text{T}} \boldsymbol{\Phi}$. We shall denote the following remarks:

- The resulting reduced matrix problem is very small due to the fact that N is supposed to be very small compared to the displacement structural degree of freedom;
- All the matrices are symmetric, according to Eq. (8), $\mathbf{r}_{\mathrm{a}} = \rho_{\mathrm{f}}\mathbf{B}^{\mathrm{T}}\mathbf{C}\mathbf{H}^{-1}\mathbf{C}^{T}\mathbf{B}$, except that no matrix inversion have been computed for $\mathbf{r}_{\mathrm{a}}$ but only N linear system of equations;
- If N is high enough, the K first eigenvalues of this reduced problem (with $K \leq N$) converge to the K first one of the hydroelastic with the full added mass matrix;
- The N linear system of equations can be done in parallel.

4 Numerical examples

The objective of the numerical examples is to compare the hydroelastic dynamic behavior computed with (i) classical added mass formulation and (ii) the coupled problem projected on the dry mode. Two cases are presented, one with prestressed effects and one without.

4.1 Example without prestressed effects of a partially filled cylinder

The first case concerns the computation of a partially filled elastic clamped cylinder with a rigid bottom (see Fig. 3 for the geometry and the mesh parameterization). The material properties are the Young modulus $E = 200 \times 10^9$ Pa, the Poisson ratio $\nu = 0.33$, the structural mass density $\rho_{\mathrm{s}} = 7.8 \times 10^3$ kg/m^3 and $\rho_{\mathrm{f}} = 1.0 \times 10^3$ kg/m^3.

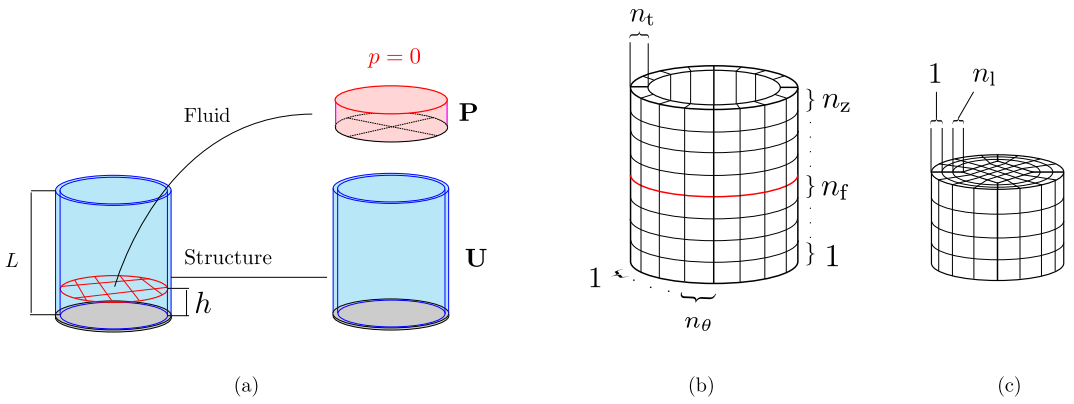

Figure 3: (a) Geometry of the partially filled elastic clamped cylinder with rigid bottom with $t = 6$ mm, $L = 6$ m and $R = 2$ m; (b) Mesh parameterization, with 20 hexaedral elements, where $n_t = 1$ and $n_l = 4$ are fixed.

The objective of this example consist to show the convergence of the problem projected on the dry modes toward the classic added mass formulation involving the computation of an inverse matrix. Three cases are analyzed :

- An empty cylinder $\tau = 0$ with $n_\theta = 10$, $n_\mathrm{z} = 10$, $n_\mathrm{f} = 0$;
- A half filled cylinder $\tau = 0.5$ with $n_\theta = 10$, $n_\mathrm{z} = 5$, $n_\mathrm{f} = 5$;
- A fully filled cylinder $\tau = 1$ with $n_\theta = 10$, $n_\mathrm{z} = 0$, $n_\mathrm{f} = 10$.

The hydroelastic analysis, done with the added mass formulation are given in Fig. 4. As expected, the natural hydroelastic frequencies rises when τ decreased.

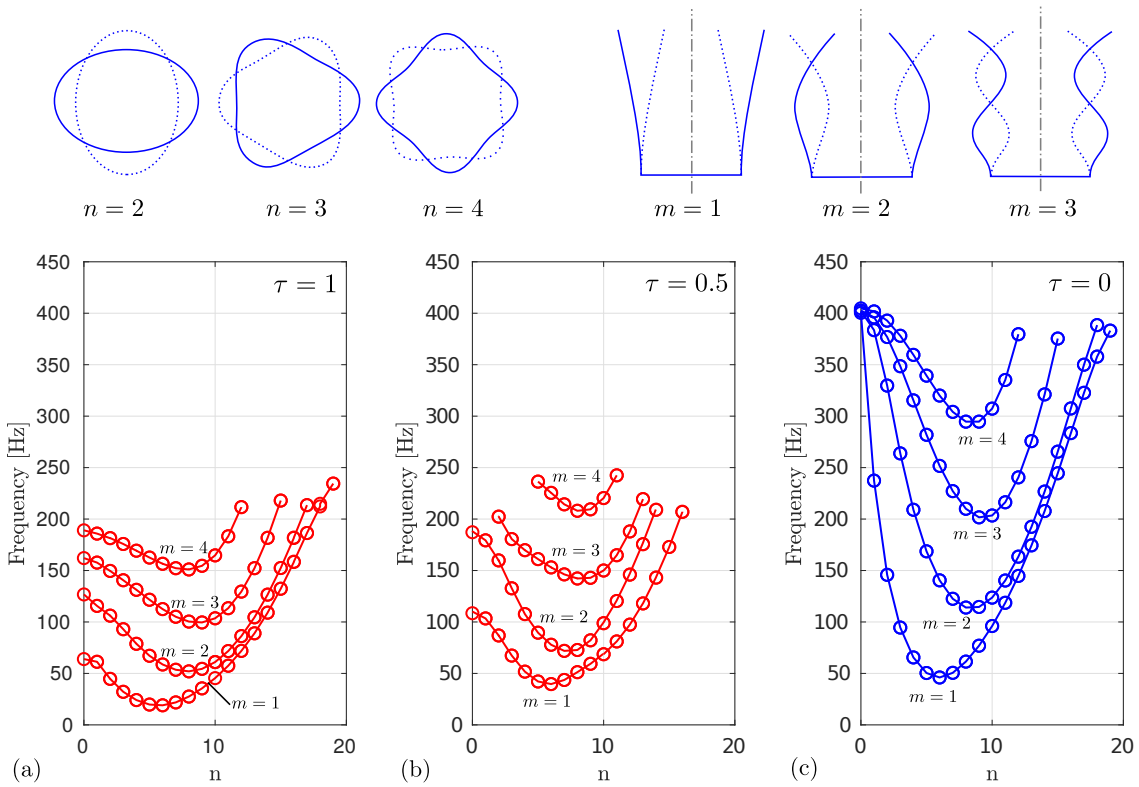

Figure 4: Representation of the circumferential and the longitudinal wave numbers n and m. (a) Hydroelastic frequencies with $\tau = 1$; ; (b) Hydroelastic frequencies with $\tau = 0.5$; (c) Natural frequencies *in vacuo*

A convergence analysis of the $K = 20$ first hydroelastic natural frequencies is presented in Fig. 5 and Fig. 6 for $\tau = 1$ and $\tau = 0.5$. For both cases the hydroelastic natural frequencies computed with the projection on N dry modes are done with $N = 20$, $N = 50$, $N = 100$ and $N = 150$:

- the proposed method based on the projection of the coupled problem on N dry modes converge toward the classic added mass formulation when N increases;

- the maximum error within the $K = 20$ hydroelastic frequencies, decreases, but not continuously. In fact, it depends on the contribution of a specifics number of modes. It means that the number of linear system of equation could be reduced if the modal contribution could be known *a priori*.

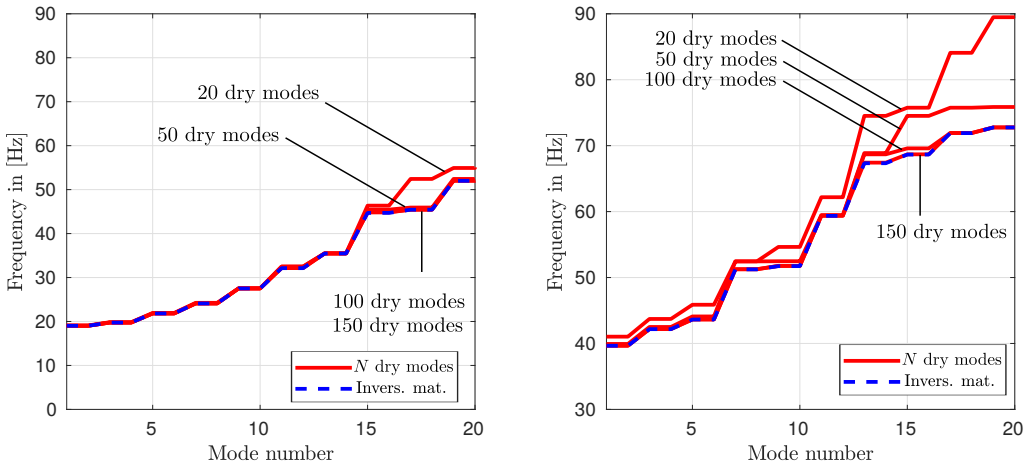

Figure 5: Value natural hydroelastic frequencies for the 20 first K modes in dashed blue (added mass formulation) and hydroelastic frequencies computed with the projection on N dry modes in red ($N = 20$, $N = 50$, $N = 100$ and $N = 150$); (a) $\tau = 1$; (b) $\tau = 0.5$.

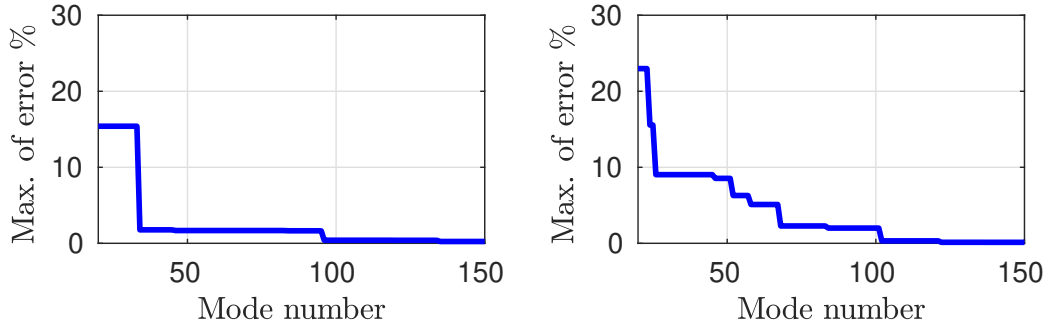

Figure 6: Evolution of the maximum error on the $K = 20$ first hydroelastic modes between the two approaches in function of the number of dry modes. The added mass formulation with the full matrix is the reference.

A comparison between computational times is done for the fully filled cylinder τ, considering various mesh parameterizations which increase the number of fluid degrees of freedom (see Tab. 1). Two computational times are considered:

- the time needed to compute $\mathbf{H}_*^{-1}$;
- the time needed to solve N linear system form Eq. (8).

(n_θ, n_f)	$(5,5)$	$(10,10)$	$(15,15)$
$n_{\text{elem-s}}$ (structure)	100	400	900
$n_{\text{elem-f}}$ (fluid)	500	2600	6975
$n_{\text{dof-s}}$ (structure)	2100	8400	18900
$n_{\text{dof-f}}$ (fluid)	2260	11020	29280

Table 1: Number of elements and number of degrees of freedom for the structure and the fluid in function of the mesh parameterization

In Fig. 7, two graphs are proposed (one for $N = 20$ and the other for $N = 150$) in which the computational time is plotted in function of the number of degrees of freedom on the fluid.

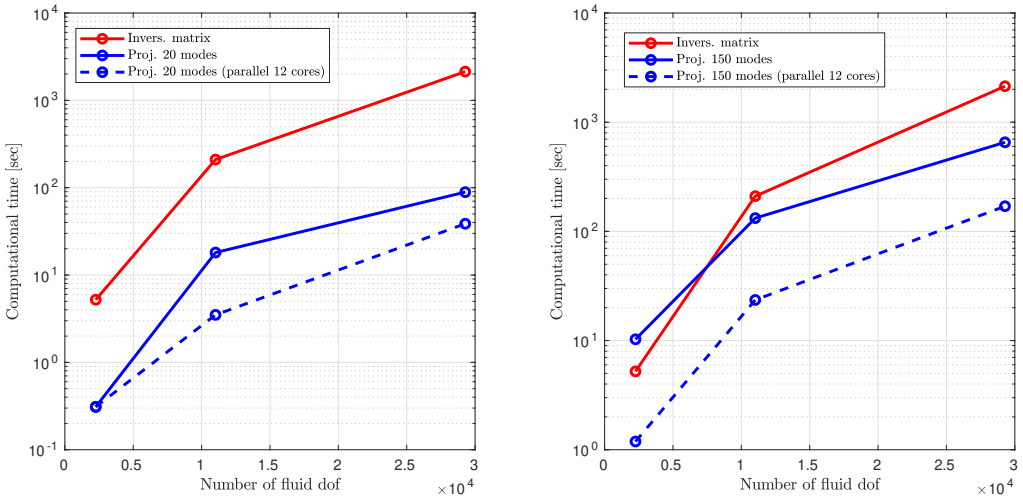

Figure 7: Computational time in function of the number of pressure degrees of freedom (in red a matrix inversion is computetd, in blue N linear system is computed one by one and in dashed blue line N linear system is done in parallel with 12 cores).

- As expected, if the number of degrees of freedom is to high, the computation time needed to inverse the matrix is prohibitive (more than 2000 second for 29280 fluid degrees of freedom);

- In the proposed approach with the projection on dry modes, N linear system of equations are computed. Except for very coarse systems, the computational time of the projection on dry modes is lower than the matrix inversion (it depend on the fluid degree of freedoms and the number N of linear system). Even if those systems can be solved in parallel, among the N contributions, it seems that only a few of them contributes to the convergence. The number of linear systems could be even more reduced.

4.2 Validation with prestressed effects

The projection on prestressed dry mode have been performed in a clamped elastic bottom based on an experiment done in [2]. The problem consists in computing the hydroelastic angular frequencies of the prestressed elastic circular plate in function of the fluid height. Geometrical nonlinearities are taken into account and have been computed before the dynamic analysis. The geometrical and mesh parameters are exposed in Fig. 8. The material parameters are $E = 5.47 \times 10^9$, $\nu = 0.38$, $\rho_\mathrm{s} = 1.4 \times 10^3$ kg/m^3 and $\rho_\mathrm{f} = 1.0 \times 10^3$ kg/m^3.

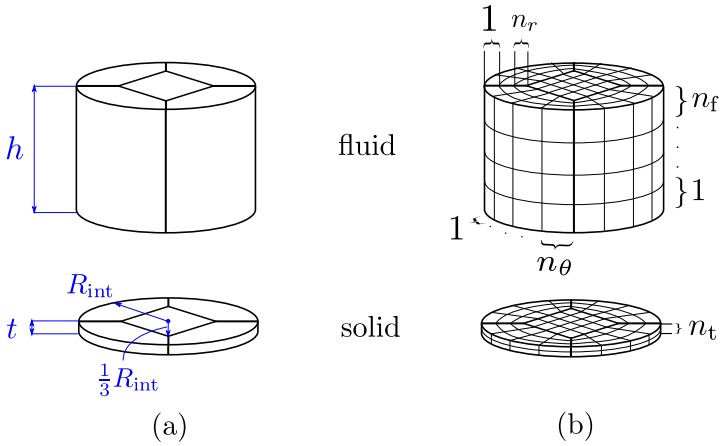

Figure 8: (a) Geometrical parameterization of the elastic bottom submetted by an hydrostatic pressure of a fluid column of height h with $R_{\mathrm{int}} = 0.144$ m and $t = 0.35$ mm; (b) Mesh parameterization, with 20 hexaedral elements, used for the computation of the hydroelastic angular frequencies with $n_\mathrm{r} = 10$, $n_\mathrm{f} = 10$, $n_\theta = 10$ $n_\mathrm{t} = 2$.

In Fig. 9, the evolution of natural angular hydroelastic frequencies are plotted between 0 and 80 Hz in function of the fluid height $h \in [0, 250]$ mm and $dh = 5$.

- 50 hydroelastic reduced eigenvalues problems have been computed by using the projection of prestressed dry modes in 1 hour;
- For each fluid height, the first $N = 25$ dry modes have been selected;

- Except for the first modes, the angular natural frequencies decrease, then increase when the fluid height increase in the given fluid height range;
- Very good agreements with the experiment is observed, compared to the literature;
- One computation of the hydroelastic angular frequencies, for a given fluide height, with the full inversion of the added mass matrix takes more than $3h$ for the same mesh parameterization.

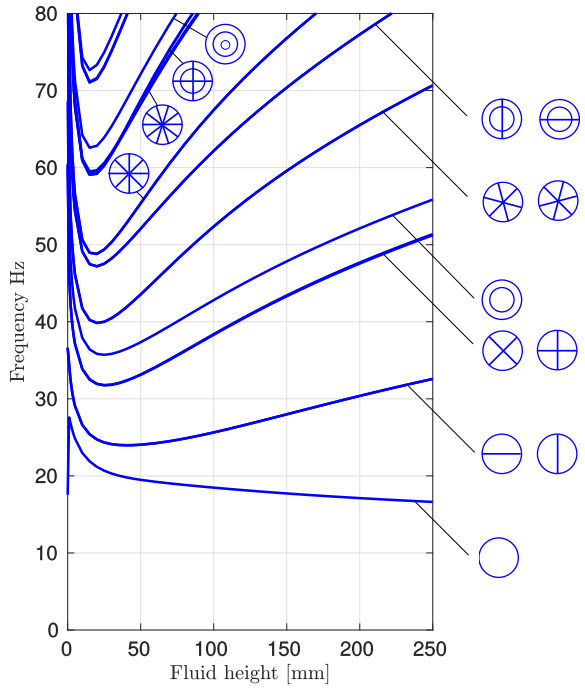

Figure 9: Evolution of the angular natural hydroelastic frequencies in function of the fluid height with $h \in [0, 250]$ mm and $dh = 5$.

5 CONCLUSIONS AND OUTLOOKS

In this paper, the computation of the linearized prestressed hydroelastic behaviour of partially filled elastic tanks have been proposed. The numerical estimation, done with the finite element method, of the prestressed effects on the fluid-structure dynamic analysis has been adressed. A methodology based on the projection of the fluid-structure problem on the structural prestressed dry modes is detailed in a discrete framework. It is shown that for a given number of hydroelastic modes, the proposed approach converges to a full

hydroelastic formulation, without computing any full matrix inverse. Consequently, the computational time is reduced. Two numerical examples are treated, one with prestressed effects and one without. Both results shows the effectiveness of the projection on a dry mode basis. Further developments are expected in the future such as the use of the approach on much more complex structures and the selection of a minimum number of dry modes needed to minimize the number of linear system that has to be solved.

REFERENCES

[1] Morand, H.-J.P. and Ohayon, R. *Fluid Structure Interaction*, John Wiley & Son, 1995.

[2] Chiba, M. Nonlinear hydroelastic vibration of a cylindrical tank with an elastic bottom, containing liquid. Part I: Experiment, *J. Fluids Struct.* (1992) **6**:181–206.

[3] Schotté, J.-S. and Ohayon, R. Various modelling levels to represent internal liquid behaviour in the vibration analysis of complex structures *Comput. Methods Appli. Mech. Engrg.* (2009) **198**:1313–1925.

[4] Hoareau, C. and Deü, J.-F. A finite element approach for hydroelastic vibrations of partially filled prestressed elastic tanks *in Proceeding of the 6th European Conference on Computational Mechanic.* (2019), ECCM6, Glasgow, UK.

[5] Haßler, M. and Schweizerhof, K. On the static interaction of fluid and gas loaded multi-chamber systems in large deformation finite element analysis *Comput. Methods Appli. Mech. Engrg.* (2009) **197**:1725–1749.